

Dark Matter Detectors as a Novel Probe for Light New Physics

Anirban Majumdar,^{1,*} D. K. Papoulias,^{2,†} and Rahul Srivastava^{1,‡}

¹*Department of Physics, Indian Institute of Science Education and Research - Bhopal,
Bhopal Bypass Road, Bhauri, Bhopal 462066, India*

²*Division of Theoretical Physics, University of Ioannina, GR 45110 Ioannina, Greece*

We explore the prospect of constraining light mediators at the next generation direct detection dark matter detectors through coherent elastic neutrino-nucleus scattering (CE ν NS) and elastic neutrino-electron scattering (E ν ES) measurements. Taking into account various details like the quenching factor corrections and atomic binding effects, we obtain the model independent projected sensitivities for all possible Lorentz invariant interactions, namely scalar (S), pseudoscalar (P), vector (V), axial vector (A) and tensor (T). For the case of vector interactions, we also focus on two concrete examples: the well-known $U(1)_{B-L}$ and $U(1)_{L_\mu-L_\tau}$ gauge symmetries. For all interaction channels $X = \{S, P, V, A, T\}$, our results imply that the upcoming dark matter detectors have the potential to place competitive constraints, improved by about one order of magnitude compared to existing ones from dedicated CE ν NS experiments, XENON1T, beam dump experiments and collider probes.

1. INTRODUCTION

Although the Standard Model (SM) provides a rather successful description of electroweak and strong interactions in nature, there is a list of shortcomings that point to the need of new physics Beyond the Standard Model (BSM). Usually it is assumed that the scale of such new physics is larger than the electroweak symmetry breaking scale and the new BSM particles are heavy. For example, the existence of new neutral Z' gauge bosons under an extra gauge symmetry is a common feature of many theories beyond the SM [1]. Extensive phenomenological studies at colliders [2] have been performed, taking the Z' bosons to be heavier than electroweak scale.

However, there exist various motivated BSM extensions where the new physics is desirable to be at the low scale. Light new physics, for example, can account for the explanation of existing anomalies such as the longstanding anomalous magnetic moment of muon [3, 4]. Moreover, concerning the dark sector, several dark matter models require the presence of

* anirban19@iiserb.ac.in

† d.papoulias@uoi.gr

‡ rahul@iiserb.ac.in

light mediators to account for dark matter self interaction [5, 6] and/or the recent XENON1T anomaly [7–9]. Finally, the Peccei-Quinn solutions of strong CP-problem also implies the presence of a light Nambu-Goldstone boson called axion [10–12], while neutrino mass models involving dynamical lepton number breaking often lead to a light pseudoscalar boson called Majoron (Majorana Neutrinos) or Diracon (Dirac neutrinos) [13, 14].

While the implications of light vector and scalar mediators to the expected signal rates had already been explored at direct detection dark matter experiments [15, 16], after the recent observation of coherent elastic neutrino-nucleus scattering ($\text{CE}\nu\text{NS}$) by the COHERENT experiment [17–19] there has been an intense interest for novel mediator investigations [20–27]. In addition to COHERENT, data-driven constraints also exist from upper limits on $\text{CE}\nu\text{NS}$, placed by the recent CONNIE [28] and CONUS [29] measurements. Phenomenological studies focusing on various $U'(1)$ realisations such as the $L_\mu - L_\tau$ and $B - L$ gauge symmetries have been explored using solar neutrinos [30, 31] as well as using supernova neutrinos taking also into account corrections from medium effects [32]. It is interesting to note that the latter can induce a reduction of the cross section due to Pauli blocking and therefore lead to less severe constraints. Very recently, the expected modification to the neutrino-floor has been illustrated in the presence of vector and scalar mediators [33], while the complementarity of $\text{CE}\nu\text{NS}$ and direct detection dark matter experiments was emphasised through a data-driven analysis of the neutrino floor.

In addition to scalar and vector mediator scenarios, it is possible to explore further Lorentz invariant structures, such as Scalar (S), Pseudoscalar (P), Vector (V), Axial Vector (A) or Tensor (T) interactions in a model independent way through Neutrino Generalized Interactions (NGIs). Assuming heavy mediators, NGIs have been explored in Ref. [34] using $\text{CE}\nu\text{NS}$ data from COHERENT and in Ref. [35] through elastic neutrino-electron scattering ($\text{E}\nu\text{ES}$) by analysing the Borexino data. Reference [36] performed a global NGI analysis in the light data from $\text{E}\nu\text{ES}$ experiments, neutrino Deep Inelastic Scattering, and single-photon detection from electron-positron collisions, while Ref. [37] pointed out the possibility of probing the Dirac or Majorana neutrino nature through NGIs. Tensorial exotic interactions have been explored in Ref. [38] using the TEXONO data as well as in Ref. [39] where their connection to neutrino transition magnetic moments was emphasised. Finally, constraints in the tensor parameter space were extracted from the analysis of COHERENT data [40] and more recently by the CONUS collaboration [29].

The next generation direct detection dark matter experiments with multi-ton mass scale and sub-keV capabilities are expected to become sensitive to astrophysical neutrinos. Indeed, the XENON1T Collaboration has already reported first results in its effort to identify a potential $\text{CE}\nu\text{NS}$ population–induced by ^8B neutrinos of the solar flux–in the background data [41]. Motivated by the upcoming large scale next generation direct detection dark

matter experiments such as XENONnT [42], in this work we consider the possibility of exploring neutrino backgrounds using nuclear and electron recoils. In particular, we are interested to explore the prospects of constraining general neutrino interactions induced by novel mediators via $\text{CE}\nu\text{NS}$ and $\text{E}\nu\text{ES}$ measurements at a future direct detection dark matter experiment. Unlike previous studies—especially for the cases of pseudoscalar, axial vector and tensor interaction channels—we allow the exchanged mediator to be sufficiently light. Therefore, for all possible interaction channels, the dependence on the mediator mass has been considered explicitly in the cross sections. Our present results indicate that future dark matter detectors will offer competitive constraints in the mass-coupling parameter space, being also complementary to collider probes and DUNE.

The remainder of the paper has been organised as follows. In Sec. 2 we provide the necessary formalism regarding $\text{CE}\nu\text{NS}$ processes. We start with the discussion of $\text{CE}\nu\text{NS}$ within SM and then discuss the new physics contribution to it. In Sec. 3 we discuss the case of $\text{E}\nu\text{ES}$, again starting with the SM discussion and ending with the new physics contribution. Our main results are presented in Sec. 4 where we first discuss the model independent constraints on various types of new physics scenarios. We then, as examples, take a few specific models with light mediators and further analyse our constraints, comparing and contrasting them with constraints obtained from other experimental probes. Our concluding remarks are summarised in Sec. 5.

2. COHERENT ELASTIC NEUTRINO NUCLEUS SCATTERING

In this section, we provide the basic formalism for the description of the various $\text{CE}\nu\text{NS}$ interaction channels considered in the present work, within and beyond the SM. A model independent analysis is performed by considering all possible Lorentz invariant interaction channels in the low energy regime. The latter can be conveniently classified in terms of the Lorentz and Parity transformations of the mediator particle i.e. whether the mediator transforms as S, P, V, A, T under Lorentz and Parity transformations. One further advantage of such parametrisation is that interactions of any particle having a mixed transformation (e.g. SM Z^0 boson) can also be taken into account simply as a combination of S, P, V, A, T interactions.

2.1. $\text{CE}\nu\text{NS}$ within the SM

Assuming SM interactions only, for low and intermediate neutrino energies ($E_\nu \ll M_{Z^0}$) $\text{CE}\nu\text{NS}$ is accurately described in the context of an effective 4-fermion Fermi interaction

Lagrangian [43]

$$\mathcal{L}_{SM} = -2\sqrt{2}G_F \sum_{\substack{f=u,d \\ \alpha=e,\mu,\tau}} g_{\alpha,\alpha}^{f,P} [\bar{\nu}_\alpha \gamma^\rho L \nu_\alpha] [\bar{f} \gamma_\rho P f] . \quad (1)$$

Here, $P \equiv \{L, R\}$ stand for the chiral projection operators, $f \equiv \{u, d\}$ represents a first generation quark and $g_{\alpha,\alpha}^{f,P}$ is the P -handed coupling of the quark f to the SM Z^0 boson. The latter are expressed in terms of the weak mixing angle ($\sin^2 \theta_W = 0.2387$), as

$$\begin{aligned} g_{\alpha,\alpha}^{u,L} &= \frac{1}{2} - \frac{2}{3} \sin^2 \theta_W , & g_{\alpha,\alpha}^{u,R} &= -\frac{2}{3} \sin^2 \theta_W , \\ g_{\alpha,\alpha}^{d,L} &= -\frac{1}{2} + \frac{1}{3} \sin^2 \theta_W , & g_{\alpha,\alpha}^{d,R} &= \frac{1}{3} \sin^2 \theta_W . \end{aligned} \quad (2)$$

At tree level¹, the SM differential CE ν NS cross section with respect to the nuclear recoil energy E_{nr} is given as [45]

$$\left[\frac{d\sigma}{dE_{nr}} \right]_{SM}^{\nu N} = \frac{G_F^2 m_N}{\pi} (Q_V^{SM})^2 \left(1 - \frac{m_N E_{nr}}{2E_\nu^2} \right) , \quad (3)$$

where m_N is the nuclear mass, while the SM vector weak charge Q_V^{SM} takes the form [46]

$$Q_V^{SM} = [g_p^V Z + g_n^V N] F_W(q^2) . \quad (4)$$

Here, Z and N denote the number of protons and neutrons in the nucleus while the corresponding vector couplings for protons (g_p^V) and neutrons (g_n^V) read [47]

$$\begin{aligned} g_p^V &= 2(g_{\alpha,\alpha}^{u,L} + g_{\alpha,\alpha}^{u,R}) + (g_{\alpha,\alpha}^{d,L} + g_{\alpha,\alpha}^{d,R}) = 1/2 - 2 \sin^2 \theta_W , \\ g_n^V &= (g_{\alpha,\alpha}^{u,L} + g_{\alpha,\alpha}^{u,R}) + 2(g_{\alpha,\alpha}^{d,L} + g_{\alpha,\alpha}^{d,R}) = -1/2 . \end{aligned} \quad (5)$$

It is noteworthy that Eq.(3) is valid for sufficiently low momentum transfer in order to satisfy the coherency condition $q \leq 1/R_A$ [46], with R_A being the nuclear radius and $q^2 = 2m_N E_{nr}$ denoting the magnitude of 3-momentum transfer. Moreover, to account for the finite nuclear spatial distribution, nuclear physics corrections are incorporated in Eq.(4) through the weak nuclear form factor $F_W(q^2)$. In our present study we adopt the Helm parametrization, given as [48]

$$F_W(q^2) = \frac{3j_1(qR_0)}{qR_0} e^{[-\frac{1}{2}(qs)^2]} , \quad (6)$$

where $j_1(x)$ is 1st-order Spherical Bessel function, while the diffraction radius is given by $R_0^2 = R^2 - 5s^2$ with the nuclear radius and surface thickness taken to be $R = 1.2 A^{1/3}$ fm

¹ Subdominant radiative corrections are discussed in Ref. [44].

and $s = 0.9$ fm, respectively.

2.2. CE ν NS contribution from Light Novel Mediators

NGIs constitute a useful model-independent probe that can accommodate several attractive BSM scenarios. By restricting ourselves to low-energy neutral-current interactions (below the electroweak symmetry breaking scale), in this work we consider general new physics interactions arising from the Lagrangian [34, 49]

$$\mathcal{L}_{NGI} = \frac{G_F}{\sqrt{2}} \sum_{\substack{X=S,P,V,A,T \\ f=u,d \\ \alpha=e,\mu,\tau}} C_{\alpha,\alpha}^{f,P} [\bar{\nu}_\alpha \Gamma^X L \nu_\alpha] [\bar{f} \Gamma_X P f] . \quad (7)$$

Therefore, in what follows all possible Lorentz-invariant structures are taken into account, i.e. $\Gamma_X = \{\mathbb{1}, i\gamma_5, \gamma_\mu, \gamma_\mu \gamma_5, \sigma_{\mu\nu}\}$ (with $\sigma_{\mu\nu} = \frac{i}{2}[\gamma_\mu, \gamma_\nu]$), corresponding to $X = \{S, P, V, A, T\}$ interactions, respectively. The dimensionless coefficients $C_{\alpha,\alpha}^{f,P}$ measure the relative strength of the new physics interaction X and are of the order of $(\sqrt{2}/G_F)(g_X^2/(q^2 + m_X^2))$ with m_X and g_X being the mass of the exchanged light mediator and the corresponding coupling, respectively. Throughout this work, we define the coupling $g_X = \sqrt{g_{\nu X} g_{fX}}$; $f = \{u, d\}$ for CE ν NS and $f = e$ for E ν ES.

We proceed by relying on previous analyses [50, 51] which, in the limit of vanishing momentum transfer, argued that the nucleonic matrix element of the quark current is proportional to that of the corresponding nucleon current $\langle N_f | \bar{q} \Gamma^X q | N_i \rangle \equiv \mathcal{F}^X(q) \langle N_f | \bar{N} \Gamma^X N | N_i \rangle$ where $\mathcal{F}^X(q)$ is the form factor calculated within the framework of non-perturbative low-energy QCD. The individual interactions and their contribution to the CE ν NS differential cross section are listed in Table I. For the different interactions X , the relevant effective charges Q_X entering the respective cross sections are given by [15, 38, 51, 52]

$$\begin{aligned} Q_s &= g_{\nu S} \left(Z \sum_q g_{qS} \frac{m_p}{m_q} f_q^p + N \sum_q g_{qS} \frac{m_n}{m_q} f_q^n \right) F_W(q^2), \\ Q_P &= g_{\nu P} \left(Z \sum_q g_{qP} \frac{m_p}{m_q} h_q^p + N \sum_q g_{qP} \frac{m_n}{m_q} h_q^n \right) F_W(q^2), \\ Q_V &= g_{\nu V} [(2g_{uV} + g_{dV}) Z + (g_{uV} + 2g_{dV}^V) N] F_W(q^2), \\ Q_A &= g_{\nu A} \left(Z S_p \sum_q g_{qA} \Delta_q^p + N S_n \sum_q g_{qA} \Delta_q^n \right) F_W(q^2), \\ Q_T &= g_{\nu T} \left(Z \sum_q g_{qT} \delta_q^p + N \sum_q g_{qT} \delta_q^n \right) F_W(q^2). \end{aligned} \quad (8)$$

Mediator	\mathcal{L}_X	Cross Section
Scalar	$\left[(g_{\nu S} \bar{\nu}_R \nu_L + h.c.) + \sum_{q=\{u,d\}} g_{qS} \bar{q} q \right] S + \frac{1}{2} m_S^2 S^2$	$\frac{m_N^2 E_{nr} Q_S^2}{4\pi E_\nu^2 (q^2 + m_S^2)^2}$
Pseudoscalar	$\left[(g_{\nu P} \bar{\nu}_R \gamma_5 \nu_L + h.c.) - i \sum_{q=\{u,d\}} g_{qP} \bar{q} \gamma_5 q \right] P + \frac{1}{2} m_P^2 P^2$	$\frac{m_N E_{nr}^2 Q_P^2}{8\pi E_\nu^2 (q^2 + m_P^2)^2}$
Vector	$\left[g_{\nu V} \bar{\nu}_L \gamma_\mu \nu_L + \sum_{q=\{u,d\}} g_{qV} \bar{q} \gamma_\mu q \right] V^\mu + \frac{1}{2} m_V^2 V^\mu V_\mu$	$\left(1 + \frac{Q_V}{\sqrt{2} G_F Q_V^{SM} (q^2 + m_V^2)} \right)^2 \left[\frac{d\sigma}{dE_{nr}} \right]_{SM}^{\nu N}$
Axial Vector	$\left[g_{\nu A} \bar{\nu}_L \gamma_\mu \gamma_5 \nu_L - \sum_{q=\{u,d\}} g_{qA} \bar{q} \gamma_\mu \gamma_5 q \right] A^\mu + \frac{1}{2} m_A^2 A^\mu A_\mu$	$\frac{m_N Q_A^2 (2E_\nu^2 + m_N E_{nr})}{4\pi E_\nu^2 (q^2 + m_A^2)^2}$
Tensor	$\left[g_{\nu T} \bar{\nu}_R \sigma_{\rho\delta} \nu_L - \sum_{q=\{u,d\}} g_{qT} \bar{q} \sigma_{\rho\delta} q \right] T^{\rho\delta} + \frac{1}{2} m_T^2 T^{\rho\delta} T_{\rho\delta}$	$\frac{m_N Q_T^2 (4E_\nu^2 - m_N E_{nr})}{2\pi E_\nu^2 (q^2 + m_T^2)^2}$

TABLE I: Novel interactions $X = \{S, P, V, A, T\}$ and corresponding differential CE ν NS cross sections considered in the present work.

In the latter expressions, the hadronic structure parameters for the scalar case (S) are: $f_u^p = 0.0208$, $f_u^n = 0.0189$, $f_d^p = 0.0411$, $f_d^n = 0.0451$ [53], for the pseudoscalar case (P) are: $h_u^p = h_u^n = 1.65$, $h_d^p = h_d^n = 0.375$ [54], and for the tensor case (T) are: $\delta_u^p = \delta_u^n = 0.54$, $\delta_d^p = \delta_d^n = -0.23$ [53]. Finally, for the case of axial vector (A) interactions the hadronic parameters read: $\Delta_u^p = \Delta_u^n = 0.842$, $\Delta_d^p = \Delta_d^n = -0.427$ [55], while the spin expectation values (S_p and S_n) are nuclear model and isotope dependent. In the present study we focus on the ^{131}Xe isotope and hence we rely on the following spin expectation values for protons ($S_p = -0.009$) and neutrons ($S_n = -0.272$), extracted from shell model nuclear structure calculations in Ref. [56].

A few comments are in order. First, from Table I it becomes evident that for the case of S, P, A, T interactions there is absence of interference with the SM CE ν NS cross section, in contrast to the vector mediator case where the new physics contribution yields interference terms. For the sake of clarity we should stress that, in principle, the axial vector interaction adds incoherently to the SM CE ν NS cross section, however the SM axial contribution is significantly suppressed with respect to the vector one, and therefore neglected (see Ref. [40]). Moreover, as discussed in Ref. [34] the existence of axial quark terms in the interaction Lagrangian (7) will lead to pseudoscalar-scalar neutrino-quark couplings, the study of which will be relaxed as it goes well beyond the scope of our work. Finally, the P and A terms are spin-dependent and therefore suppressed with respect to S, V, T terms². For the latter issue, we will rely on the assumption that the new physics interaction is controlled by the strength of the neutrino coupling.

Focusing on light vector mediators only, in this work we will consider three different models, determined by the charges of leptons Q'_ℓ and quarks Q'_q under the extra gauge symmetry $U(1)'$ [59]. First, we consider a generic model where the new vector mediator V couples universally to all SM fermions, such that $Q'_\ell = Q'_q = 1$, corresponding to an effective

² In Ref. [15] the P contribution to CE ν NS was reported to be vanishing based on the fact that the corresponding nucleon matrix element is vanishing [57, 58].

vector charge in Eq.(8) with $g_{qV} = g_{\nu V}$. Secondly, we focus on the U_{B-L} extension of the SM, in which the anomaly cancellation conditions $Q'_\ell = -1$, $Q'_q = 1/3$ imply an effective vector charge with $g_{qV} = -g_{\nu V}/3$. Finally, we consider the gauged $U_{L_\mu-L_\tau}$ symmetry, where the new vector mediator boson couples directly only to muons and taus with absence of tree-level couplings to quarks. In this model, contributions to CE ν NS are possible at the 1-loop level, through kinetic mixing between the new mediator and the SM photon [60] and the corresponding cross section reads [27]

$$\left[\frac{d\sigma}{dE_{nr}} \right]_{L_\mu-L_\tau}^{\nu N} = \left(1 \pm \frac{\alpha_{em} g_{\nu V} g_{qV} \log\left(\frac{m_\tau^2}{m_\mu^2}\right) ZF(q^2)}{3\sqrt{2}\pi G_F Q_V^{SM} (q^2 + m_V^2)} \right)^2 \left[\frac{d\sigma}{dE_{nr}} \right]_{SM}^{\nu N}, \quad (9)$$

where α_{em} is fine structure constant, while m_μ and m_τ denote the muon and tau masses, respectively³, while the plus (minus) sign accounts for ν_τ -nucleus (ν_μ -nucleus) scattering.

3. ELASTIC NEUTRINO ELECTRON SCATTERING

Proceeding in an analogous way as in the case of CE ν NS, in this section we discuss the formalism describing E ν ES within and beyond the SM.

3.1. E ν ES through SM Interaction Channel

E ν ES is a well-understood weak flavoured process where (anti-)neutrinos of flavour $\alpha = \{e, \mu, \tau\}$ interact with electrons via elastic scattering at low and intermediate energies, receiving contributions from both neutral- and charged-current for $\alpha = e$, and neutral-current only for $\alpha = \{\mu, \tau\}$. Within the framework of the SM, the corresponding Lagrangian density corresponding to the process $\bar{\nu}_e^{(-)} + e^- \rightarrow \bar{\nu}_e^{(-)} + e^-$, reads⁴ [62]

$$\begin{aligned} \mathcal{L}_{SM}(\bar{\nu}_e^{(-)} + e^- \rightarrow \bar{\nu}_e^{(-)} + e^-) = & -\frac{G_F}{\sqrt{2}} \{ [\bar{\nu}_e \gamma^\rho (1 - \gamma_5) e] [\bar{e} \gamma_\rho (1 - \gamma_5) \nu_e] \\ & + [\bar{\nu}_e \gamma^\rho (1 - \gamma_5) \nu_e] [\bar{e} \gamma_\rho (g_V - g_A \gamma_5) e] \}, \end{aligned} \quad (10)$$

³ For a study focusing on models with an extra $U_{B-2L_\alpha-L_\beta}$ and U_{B-3L_α} gauge symmetry, see Ref. [61].

⁴ For the case of $\nu_{\mu,\tau}-e^-$ E ν ES the Lagrangian involves only neutral-current terms.

while at the tree level the corresponding differential cross section with respect to the electron recoil energy E_{er} , is given as [63]

$$\left[\frac{d\sigma}{dE_{er}} \right]_{SM} = \frac{G_F^2 m_e}{2\pi} [(g_V + g_A)^2 + (g_V - g_A)^2 \left(1 - \frac{E_{er}}{E_\nu}\right)^2 - (g_V^2 - g_A^2) \frac{m_e E_{er}}{E_\nu^2}]. \quad (11)$$

In Eq.(11), g_V and g_A are vector and axial vector couplings respectively and take the form

$$g_V = -\frac{1}{2} + 2 \sin^2 \theta_W + \delta_{\alpha e}, \quad g_A = -\frac{1}{2} + \delta_{\alpha e}, \quad (12)$$

where the $\delta_{\alpha e}$ term is present only for $\nu_e e^-$ interactions. For the case of antineutrino scattering, the $E\nu$ ES cross section is given by Eq.(11) with the substitution $g_A \rightarrow -g_A$.

3.2. $E\nu$ ES through Light Novel Mediators

Similar to the $CE\nu$ NS case, here also we consider all possible $E\nu$ ES contributions arising from the Lorentz invariant forms $X = \{S, P, V, A, T\}$. For light vector and axial vector novel mediators, the total differential cross sections can be achieved by replacing g_V and g_A from the SM cross section as [64, 65]

$$g'_{V/A} = g_{V/A} + \frac{g_{\nu V/A} \cdot g_{eV/A}}{4\sqrt{2}G_F(2m_e E_{er} + m_{V/A}^2)}. \quad (13)$$

It is interesting to notice that in the U_{B-L} gauge extension the cross section is also given by Eq.(13) since $Q'_\ell = Q'_\nu = -1$ while in the universal case it holds that $Q'_\ell = Q'_\nu = 1$, hence both cases leading to $g_{\nu V/A} = g_{eV/A}$ in Eq.(13). On the other hand, under $U_{L_\mu-L_\tau}$ symmetry, the new light vector mediator contributes at 1-loop level for $\sigma_{\nu_\mu-e}$ and $\sigma_{\nu_\tau-e}$ only, while σ_{ν_e-e} is vanishing⁵. The relevant couplings read [60]

$$g'_V = g_V \pm \frac{\alpha_{em}}{3\sqrt{2}\pi G_F} \log\left(\frac{m_\tau^2}{m_\mu^2}\right) \frac{g_{\nu V} \cdot g_{eV}}{(2m_e E_{er} + m_V^2)}, \quad (14)$$

where, as in the $CE\nu$ NS case, the plus (minus) sign corresponds to $\sigma_{\nu_\tau-e}$ ($\sigma_{\nu_\mu-e}$) scattering. The remaining S , P and T cross section contributions add incoherently to the SM cross section and have been previously written as [9, 66]

$$\left[\frac{d\sigma}{dE_{er}} \right]_S^{\nu e} = \left[\frac{g_{\nu S}^2 \cdot g_{eS}^2}{4\pi(2m_e E_{er} + m_S^2)^2} \right] \frac{m_e^2 E_{er}}{E_\nu^2}, \quad (15)$$

⁵ Non-zero couplings contribute to σ_{ν_e-e} at 2-loop level through $Z_0 - V$ mixing which are neglected in this work.

Component	E_ν^{max} (MeV)	Flux ($\text{cm}^{-2}\text{s}^{-1}$)
pp	0.42341	5.98×10^{10}
pep	1.44	1.44×10^8
${}^7\text{Be}_{\text{High}}$	0.8613	4.99×10^9
${}^7\text{Be}_{\text{Low}}$	0.3843	4.84×10^8
${}^8\text{B}$	16.36	5.29×10^6
hep	18.784	7.98×10^3
${}^{13}\text{N}$	1.199	2.78×10^8
${}^{15}\text{O}$	1.732	2.05×10^8
${}^{17}\text{F}$	1.74	5.29×10^6
atm.	981.75	10.5
DSN	91.201	107.5

TABLE II: Neutrino endpoint energy and flux normalisation for the different astrophysical neutrino sources. The flux normalizations are taken from Ref. [73].

$$\left[\frac{d\sigma}{dE_{er}} \right]_P^{\nu e} = \left(\frac{g_{\nu P}^2 \cdot g_{eP}^2}{8\pi(2m_e E_{er} + m_P^2)^2} \right) \frac{m_e E_{er}^2}{E_\nu^2}, \quad (16)$$

$$\left[\frac{d\sigma}{dE_{er}} \right]_T^{\nu e} = \frac{m_e \cdot g_{\nu T}^2 \cdot g_{eT}^2}{2\pi(2m_e E_{er} + m_T^2)^2} \cdot \left[1 + 2 \left(1 - \frac{E_{er}}{E_\nu} \right) + \left(1 - \frac{E_{er}}{E_\nu} \right)^2 - \frac{m_e E_{er}}{E_\nu^2} \right]. \quad (17)$$

4. RESULTS

4.1. $\text{CE}\nu\text{NS}$ and $\text{E}\nu\text{ES}$ events at direct detection dark matter detectors

In our analysis we consider astrophysical neutrinos coming from the sun [67], the atmosphere [68] and from diffuse supernovae (DSN) [69]. In our calculations we have neglected the neutrino contributions coming from Geoneutrinos, as their induced events are expected to be overshadowed by several orders of magnitude with respect to solar neutrinos [70–72]. For the normalisation of the different neutrino fluxes we use the recommended conventions reported in Ref. [73] which are listed in Table II.

For the interaction channel X , the differential event rate of $\text{CE}\nu\text{NS}$ at a given detector follows from the convolution of the differential cross section with the neutrino energy distribution $d\Phi/dE_\nu$, as⁶ [46]

$$\left[\frac{dR}{dE_{nr}} \right]_X = t_{run} N_{target} \sum_i \int_{E_\nu^{min}}^{E_\nu^{max}} dE_\nu \frac{d\Phi_i(E_\nu)}{dE_\nu} \left[\frac{d\sigma}{dE_{nr}}(E_\nu, E_{nr}) \right]_X^{\nu N}, \quad (18)$$

⁶ An ideal detector with perfect efficiency and resolution power is assumed.

where t_{run} denotes the exposure time and N_{target} represents the number of target nuclei. In the latter expression, the index i runs over all the background neutrino sources with energy distribution $d\Phi_i/dE_\nu$ and E_ν^{max} denotes the maximum neutrino energy of the i -th source (see Table II). Finally, the minimum neutrino energy E_ν^{min} required to generate a nuclear recoil with energy E_{nr} is trivially obtained from the kinematics of the process and reads

$$E_\nu^{min} = \frac{m_N E_{nr}}{\sqrt{E_{nr}^2 + 2m_N E_{nr} - 2E_{nr}}} \approx \sqrt{\frac{m_N E_{nr}}{2}}. \quad (19)$$

In our analysis we also consider corrections from detector-specific quantities. In particular, for the ionisation xenon detectors considered here, a significant amount of nuclear recoil energy E_{nr} is lost into heat and other dissipative energies, so that the actual energy measured by the detector is an *electron equivalent* energy E_{er} [74]. In our calculation this effect is taken into account through the quenching factor $\mathcal{Q}_f(E_{nr})$, calculated on the basis of theoretical predictions within Lindhard theory [75]

$$\frac{E_{er}}{E_{nr}} = \mathcal{Q}_f(E_{nr}) = \frac{kg(\gamma)}{1 + kg(\gamma)}, \quad (20)$$

where $g(\gamma) = 3\gamma^{0.15} + 0.7\gamma^{0.6} + \gamma$, with $\gamma = 11.5 \cdot Z^{-\frac{7}{3}} E_{nr} (\text{keV}_{nr})$ and $k = 0.133 \cdot Z^{-\frac{2}{3}} A^{-\frac{1}{2}}$. Let us stress that for the case of germanium, low-energy corrections to the quenching factor can be accounted for through the adiabatic correction of Lindhard theory, introduced in Ref. [76]⁷. After incorporating the quenching factor corrections, the number of events in the j -th bin is written as

$$R_j = \int_{E_{er}^j}^{E_{er}^{j+1}} dE_{er} \frac{dR}{dE_{nr}} \frac{1}{\mathcal{Q}_f} \left(1 - \frac{E_{er}}{\mathcal{Q}_f} \frac{d\mathcal{Q}_f}{dE_{er}} \right). \quad (21)$$

At this point we turn our attention to $\text{E}\nu\text{ES}$. For the case of solar neutrinos the differential number of events takes into account the effect of neutrino oscillations in propagation and is given according to the expression [78]

$$\left[\frac{dR}{dE_{er}} \right]_X = t_{run} N_{target} \sum_{i=\text{solar}} \int_{E_\nu^{min}}^{E_\nu^{max}} dE_\nu \frac{d\Phi_i^{\nu_e}(E_\nu)}{dE_\nu} \left[P_{ee} \left(\frac{d\sigma_{\nu_e}}{dE_{er}} \right)_X + \overline{P}_{ef} \left(\frac{d\sigma_{\nu_f}}{dE_{er}} \right)_X \right], \quad (22)$$

⁷ Due to the lack of data for the xenon isotope we are interested in this work, we have verified that our results remain unaffected even when considering $\pm 1\sigma$ deviations from the adiabatic parameter corresponding to germanium (see table I of Ref. [76]). Improved quenching factors at sub-keV energies are comprehensively discussed in Ref. [77].

State	sp (eV)	State	sp (eV)	State	sp (eV)	State	sp (eV)
$1s_{\frac{1}{2}}$	34759.3	$3p_{\frac{3}{2}}$	1024.8	$4p_{\frac{3}{2}}$	708.1	$5p_{\frac{1}{2}}$	13.4
$2s_{\frac{1}{2}}$	5509.8	$3p_{\frac{1}{2}}$	961.2	$4p_{\frac{1}{2}}$	162.8	$5p_{\frac{3}{2}}$	12.0
$2p_{\frac{3}{2}}$	5161.5	$3d_{\frac{5}{2}}$	708.1	$4d_{\frac{5}{2}}$	73.8		
$2p_{\frac{1}{2}}$	4835.6	$3d_{\frac{3}{2}}$	694.9	$4d_{\frac{3}{2}}$	71.7		
$3s_{\frac{1}{2}}$	1170.5	$4s_{\frac{1}{2}}$	229.4	$5s_{\frac{1}{2}}$	27.5		

TABLE III: Single particle (sp) energies for the Xenon atom derived from Hartree-Fock calculations in Ref. [81].

with the minimum neutrino energy being

$$E_{\nu}^{min} = \frac{1}{2} \left[E_{er} + \sqrt{E_{er}^2 + 2m_e E_{er}} \right]. \quad (23)$$

Since the $E\nu$ ES cross section is not flavor blind as the $CE\nu$ NS one, Eq.(22) incorporates neutrino oscillations by weighting the flavoured cross section with the corresponding oscillation probability. For our purposes it is sufficient to consider the averaged oscillation probability $P_{ee}(E_{\nu})$ in the 2-flavour approximation, which we take from [79]. Notice that in the second term of Eq.(22) the oscillation factors read $\overline{P_{e\mu}} \equiv (1 - P_{ee}) \cos^2 \theta_{23}$ and $\overline{P_{e\tau}} \equiv (1 - P_{ee}) \sin^2 \theta_{23}$ for incoming ν_{μ} and ν_{τ} neutrinos, respectively⁸. Let us note that for the case of atmospheric and DSN neutrinos, oscillation effects are neglected. This is a reasonable approximation given the fact that the expected $E\nu$ ES event rates from atmospheric and DSN neutrinos are suppressed by several orders of magnitude compared to the dominant solar ones (see the discussion below). Therefore in our statistical analysis this approximation is not expected to have any quantitative effect. The differential number of $E\nu$ ES events relevant to atmospheric and DSN neutrinos is then calculated as

$$\left[\frac{dR}{dE_{er}} \right]_X = t_{run} N_{target} \sum_{i=\text{atm,DSN}} \int_{E_{\nu}^{min}}^{E_{\nu}^{max}} dE_{\nu} \frac{d\Phi_i^{\nu_{\alpha}}(E_{\nu})}{dE_{\nu}} \left(\frac{d\sigma_{\nu_{\alpha}}}{dE_{er}} \right)_X, \quad \nu_{\alpha} = \{\nu_e, \bar{\nu}_e, \nu_{\mu,\tau}, \bar{\nu}_{\mu,\tau}\}. \quad (24)$$

Up to this point, for all $E\nu$ ES interaction channels within and beyond the SM, our discussion applies to the case where neutrinos scatter off free electrons. However, the target electrons are not free, but rather bounded inside the atom. Therefore, in order to perform realistic simulations of the expected number of events at a given detector, atomic binding effects should be also considered. To account for binding effects in our analysis, the free $E\nu$ ES cross section $(d\sigma/dE_{er})_{\text{free}}$ is weighted by a series of step functions introduced in

⁸ The value of the mixing angle is taken from the best fit of the 2020 Valencia global-fit [80].

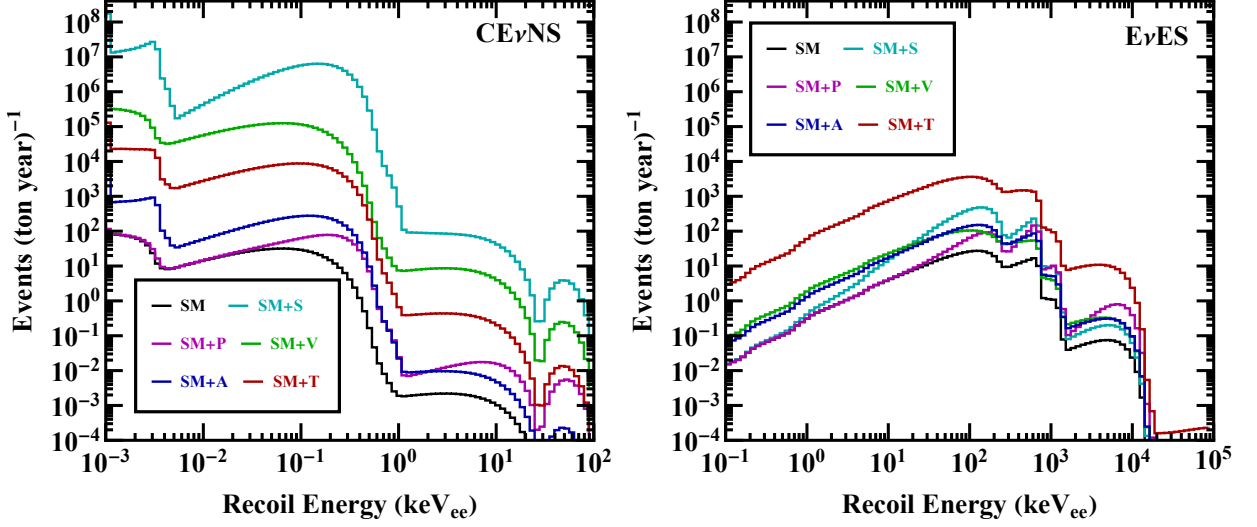


FIG. 1: Integrated event spectra expected at a xenon target for $\text{CE}\nu\text{NS}$ and $\text{E}\nu\text{ES}$ processes as a function of the recoil energy measured in keV_{ee} units. The contributions from the different new physics interactions X are calculated assuming the benchmark values $g_X^2 = 10^{-4}$ and $m_X = 1$ GeV (for details see the text).

Ref. [81] as follows

$$\frac{d\sigma}{dE_{er}} = \frac{1}{Z} \sum_{i=1}^z \Theta(E_{er} - B_i) \left(\frac{d\sigma}{E_{er}} \right)_{\text{free}}. \quad (25)$$

Here, $\Theta(x)$ is the Heaviside step function, while the quantity $\sum_{i=1}^Z \Theta(E_{er} - B_i)$ quantifies the number of electrons that can be ionised by the recoil energy E_{er} and B_i represent the binding energy of i -th electron in the atom. The single particle atomic level binding energy of electrons in ^{131}Xe atom is given in Table III [81].

Assuming typical benchmark values $g_X^2 = 10^{-4}$ and $m_X = 1$ GeV, integrated $\text{CE}\nu\text{NS}$ ($\text{E}\nu\text{ES}$) event rates for a xenon target (assuming average isotopic abundance) are shown in the left (right) panel of Fig. 1 as functions of the recoil energy for all possible interactions X . It is interesting to notice that, in general, the $\text{CE}\nu\text{NS}$ number of events are expected to exceed the $\text{E}\nu\text{ES}$ rate by several orders of magnitude. However, for a realistic next generation experiment operating with typical threshold energies i.e. $E_{er} > 0.1 \text{ keV}_{\text{ee}}$, this is not strictly true. First, for $E_{er} > 0.1 \text{ keV}_{\text{ee}}$ it becomes evident that $\text{CE}\nu\text{NS}$ -induced events will be dominated by ^8B neutrinos while the $\text{E}\nu\text{ES}$ ones will be dominated by pp neutrinos. Then, from a closer inspection of the two graphs it can be deduced that $\text{CE}\nu\text{NS}$ and $\text{E}\nu\text{ES}$ are expected to generate a comparable number of events (at least) within the SM. This can be understood as follows. Although the $\text{CE}\nu\text{NS}$ cross section scales with $\sim N^2$ as a consequence of the coherency in neutrino-nucleus scattering, the $\text{E}\nu\text{ES}$ -induced number of events is enhanced by an overall multiplicative factor Z coming due to the number of

electron targets, while the remaining difference which is of the order of an overall factor $\sim N$, is compensated by the relative difference of ^8B and pp flux normalisation. Before closing this discussion, let us note the impact of nuclear (atomic) effects in the $\text{CE}\nu\text{NS}$ ($\text{E}\nu\text{ES}$) rates. In particular, as can be seen from the $\text{CE}\nu\text{NS}$ spectral rates, there is a dip which occurs at about $25 \text{ keV}_{\text{ee}}$ corresponding to the first minimum of the nuclear form factor (see Fig. 3 of Ref. [82]), while the slight suppression of the $\text{E}\nu\text{ES}$ rates occurring for recoil energies below $1 \text{ keV}_{\text{ee}}$ reflects the atomic binding effects.

4.2. Sensitivity on S, P, V, A, T interactions

At this point we are interested to explore the projected sensitivities on the (m_X, g_X) parameter space at a typical next generation experiment looking for direct detection of dark matter. In what follows, as a representative case study we will assume a xenon detector with a $1 \text{ ton} \cdot \text{yr}$ exposure (see the discussion above). This is a conservative choice which exceeds slightly the $0.65 \text{ ton} \cdot \text{yr}$ achieved by XENON1T [83] and by a factor 20 less than the exposure goal of $20 \text{ ton} \cdot \text{yr}$ at XENONnT [42]. For our present analysis we stick to the conservative scenario described above to avoid potential overestimation of our projected sensitivities, since detector efficiency and energy resolution are not taken into consideration due to lack of information.

For estimating the projected sensitivities of the next generation experiments to the various new interaction channels $X = \{S, P, V, A, T\}$ we perform a spectral fit in terms of the χ^2 function

$$\chi^2(g_X, m_X) = \sum_{i=1}^{100} \left(\frac{R_{SM}^i - [1 + a]R_X^i(g_X, m_X)}{\sigma_{\text{stat}}^i} \right)^2 + \left(\frac{a}{\sigma_{\text{sys}}} \right)^2. \quad (26)$$

Here, the systematic uncertainty is defined as $\sigma_{\text{stat}}^i = \sqrt{R_{SM}^i + R_{bg}^i}$ where the number of background events is taken to be $R_{bg} = \sigma_{bg} R_{SM}$, while a denotes a nuisance parameter to account for the various systematic uncertainties. The systematic and background uncertainties considered in the present analysis read $\sigma_{\text{sys}} = \sigma_{bg} = 10\%$. For our spectral fit we consider 100 log-spaced bins in the range $(0.1, 100) \text{ keV}_{\text{ee}}$ for the case of $\text{CE}\nu\text{NS}$ and in the range $(0.1, 10^4) \text{ keV}_{\text{ee}}$ for the case of $\text{E}\nu\text{ES}$. Let us finally stress that in our $\text{E}\nu\text{ES}$ -based statistical analysis, the atmospheric and DSN fluxes are safely neglected. Indeed, this is a reasonable approximation given the expected SM event rates depicted in the right panel of Fig. 1.

The resulting projected sensitivities in the (m_X, g_X) parameter space are illustrated at 90% C.L. in the left and right panels of Fig. 2, respectively. As can be seen, in a future $\text{CE}\nu\text{NS}$ ($\text{E}\nu\text{ES}$) measurement among the different interaction channels the scalar (tensor)

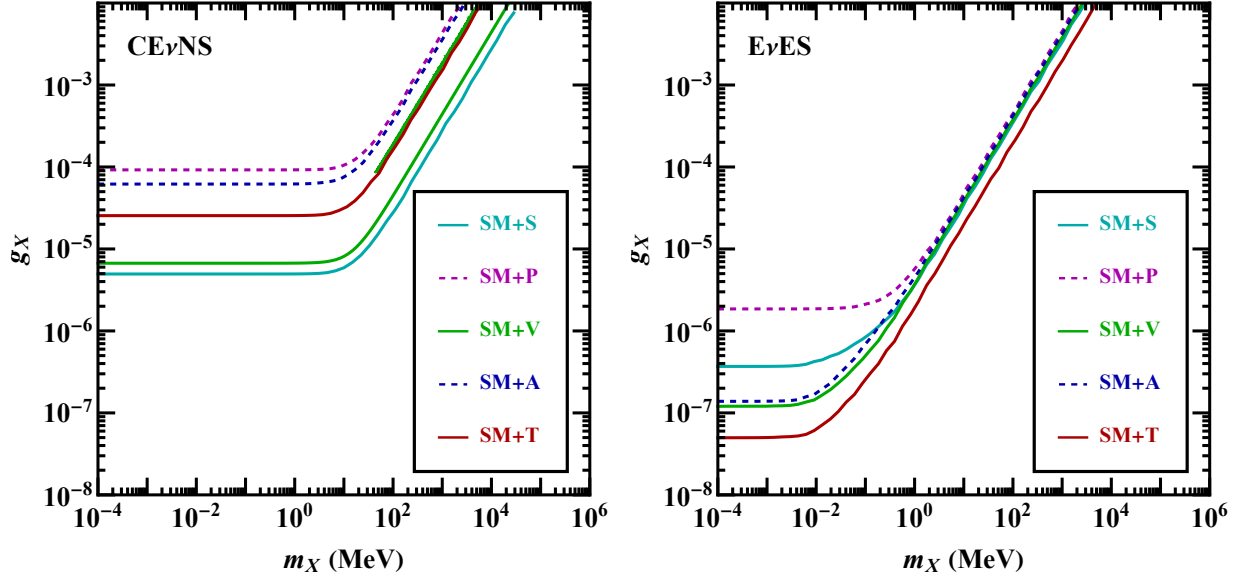


FIG. 2: Projected sensitivities for the various $X = \{S, P, V, A, T\}$ interactions for $\text{CE}\nu\text{NS}$ (left) and $\text{E}\nu\text{ES}$ (right). The results are presented at 90% C.L.

interaction will be constrained with maximum sensitivity, while for both $\text{CE}\nu\text{NS}$ and $\text{E}\nu\text{ES}$ the pseudoscalar interaction will be the least constrained. A direct comparison of $\text{CE}\nu\text{NS}$ and $\text{E}\nu\text{ES}$ sensitivities leads to the conclusion that future $\text{E}\nu\text{ES}$ measurements will be a more powerful probe for the investigation of novel light mediators. At this point it is interesting to compare our projected sensitivities with existing constraints in the literature. First, by focusing on the universal light vector mediator scenario, in the left panel of Fig. 3 we compare our present results at 90% C.L. with existing constraints from the analysis of COHERENT-CsI data [23] as well as with constraints coming from the recent CONNIE [28] and CONUS [29] data and the anomalous magnetic moment of the muon reported in Ref. [4]. Also shown are the corresponding 90% C.L. constraints coming from the XENON1T excess using $\text{E}\nu\text{ES}$ [8]. As can be seen, the latter constraints will be overridden by the future $\text{CE}\nu\text{NS}$ measurements at direct detection dark matter detectors. Finally, it becomes evident that the $\text{E}\nu\text{ES}$ channel dominates over $\text{CE}\nu\text{NS}$ in the low mass region for $m_V \leq 2\text{MeV}$.

Similar conclusions are drawn for the case of a scalar mediator, as shown in the right panel of Fig. 3. Available results can be found from $\text{CE}\nu\text{NS}$ analyses in Refs. [23, 28, 29] and from the interpretation of the XENON1T excess in Ref. [7]. Regarding the cases of S, V, A interactions for both $\text{CE}\nu\text{NS}$ and $\text{E}\nu\text{ES}$ channels as well as for the case of P using $\text{E}\nu\text{ES}$ only, similar results were found in Ref. [15]. Let us note, however, that in the latter work the sensitivities were obtained by assuming different experimental configurations as well as by neglecting quenching and atomic effects for $\text{CE}\nu\text{NS}$ and $\text{E}\nu\text{ES}$ respectively. Finally, to the best of our knowledge, regarding the cases of P and T interactions, preliminary results

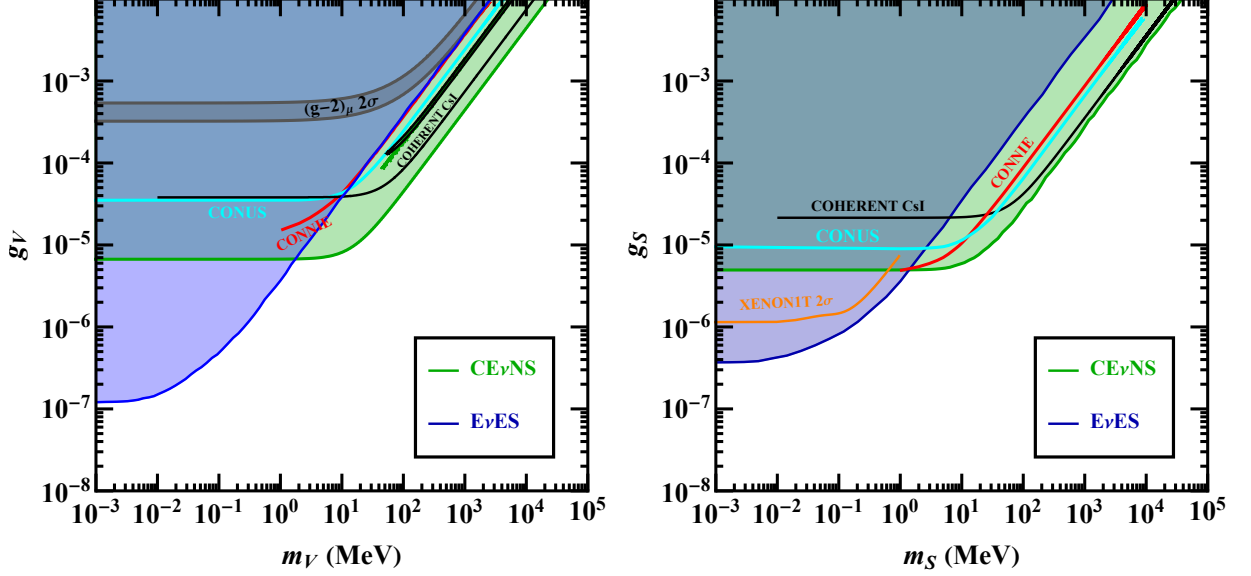


FIG. 3: Projected sensitivity at 90% C.L. in the parameter space (m_V, g_V) for the universal vector mediator model (left) and in (m_S, g_S) for a scalar mediator model (right). A comparison is given with existing constraints from dedicated CE ν NS experiments and XENON1T (see the text).

have been presented in Ref. [52] by analysing the COHERENT data. Again, the future sensitivities discussed here are about one order of magnitude more stringent than other studies.

We finally turn our attention to the vector mediator interactions predicted within the U_{B-L} and $U_{L_\mu-L_\tau}$ gauge extensions. Before proceeding with the discussion of our statistical analysis, let us provide some clarifications regarding the calculation of the number of CE ν NS and E ν ES events within the $L_\mu - L_\tau$ model. Since the $\nu_e - e^-$ coupling is vanishing, we neglect the first term in Eq.(22) and therefore a large portion of the solar neutrino flux will not contribute to the expected E ν ES rates. Likewise, in our CE ν NS-based analysis we consider only the oscillated $\nu_{\mu,\tau}$ fluxes of solar neutrinos, while from the atmospheric neutrino flux we consider only the relevant ν_μ and $\bar{\nu}_\mu$ components. For atmospheric neutrinos with sub-GeV neutrinos, matter-oscillation effects are negligible [84]. Following the procedure of Ref. [78] one sees that the oscillated fluxes reaching the detector are: $\Phi_{\text{atm}}^{\nu_e} \approx \tilde{\Phi}_{\text{atm}}^{\nu_e}$, $\Phi_{\text{atm}}^{\nu_\mu} \approx 2/3 \tilde{\Phi}_{\text{atm}}^{\nu_\mu}$ and $\Phi_{\text{atm}}^{\nu_\tau} \approx 1/3 \tilde{\Phi}_{\text{atm}}^{\nu_\mu}$, where $\tilde{\Phi}_{\text{atm}}^{\nu_\alpha}$ denotes the unoscillated flux reported in Ref. [68]. We have verified that our results remain unaffected when atmospheric neutrino oscillations are explicitly taken into account. Finally, regarding the DSN neutrino flux we assume that roughly $\Phi_{\text{DSN}}^{\nu_\mu + \bar{\nu}_\mu} \approx \Phi_{\text{DSN}}^{\nu_\tau + \bar{\nu}_\tau}$.

Left and right panels of Fig. 4 illustrate the projected sensitivity at 90% C.L. for the studied $B - L$ and $L_\mu - L_\tau$ model, respectively. The results are shown for both CE ν NS and

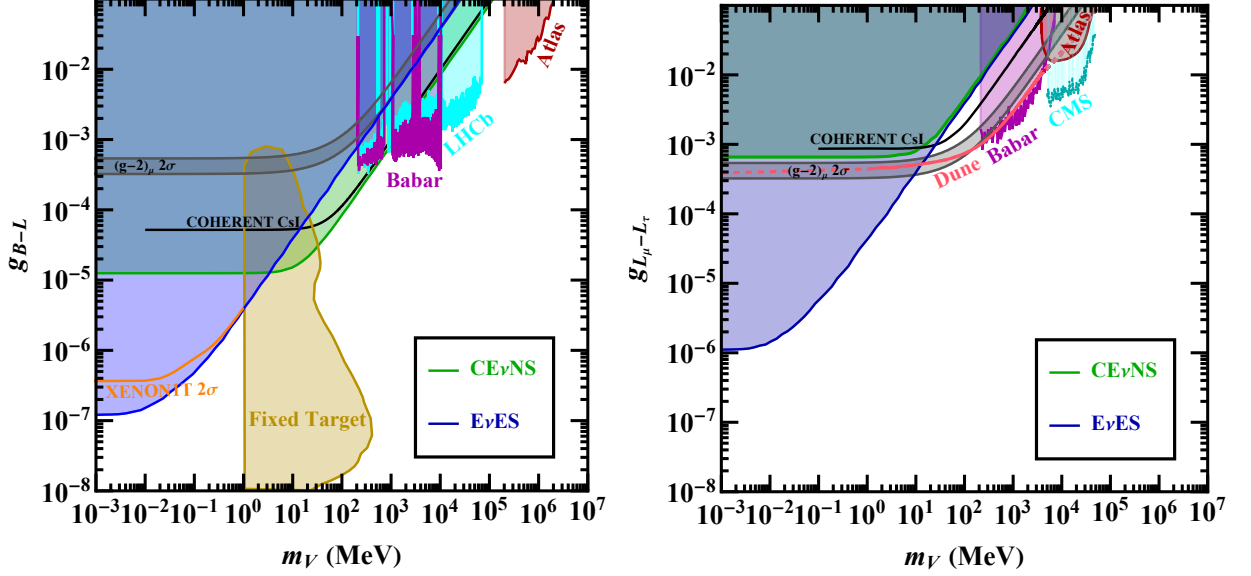


FIG. 4: Projected exclusion curves at 90% C.L. obtained in the present work using CE ν NS and E ν ES for the $B - L$ (left) and $L_\mu - L_\tau$ (right) model. A comparison with relevant experimental constraints is also given (see the text).

E ν ES at a future dark matter direct detection experiment with the same general conclusions as discussed previously. Moreover, as expected, the exclusion curves corresponding to the $B - L$ model are more stringent. In order to compare with other experimental probes, existing limits placed by dielectron resonances at ATLAS [85], electron beam-dump fixed target experiments [86, 87] as well as Dark Photon searches at BaBar [88, 89] and LHCb [90], are superimposed. Also shown are constraints derived from the analysis of the COHERENT data [27] and the XENON1T excess [8]. As can be seen, our projected sensitivities for CE ν NS dominate in mass range $0.1 \leq m_V \leq 1$ GeV, being complementary to Babar and fixed target experiments. In the same vein, our projected sensitivities obtained using E ν ES, are complementary to fixed target experiments and particularly relevant for $m_V \leq 1$ MeV.

Before closing, we should stress that astrophysics and cosmology might place severe bounds to scalar and vector interactions [22]. Those follow mostly from cosmological limits on the sum of neutrino masses, SN/stellar-cooling arguments and sterile neutrino trapping as detailed in Refs. [8, 25]. Given the large astrophysical uncertainties, such constraints should be considered as order of magnitude estimations while possible mechanisms to evade them are explained in Ref. [25]. Finally, it should be noted that upcoming experiments also have the potential to probe light mediator particles. However, our results provide about an order of magnitude more constrained bounds than those predicted for other future experiments such as neutrino trident interactions at DUNE [60], model dependent constraints for DARWIN [31] and constraints extracted from missing energy searches at NA64 μ [31].

5. CONCLUSIONS

The new era of direct dark matter experiments with multi-ton mass scale and sub-keV operation threshold makes them favourable facilities with promising prospects for detecting astrophysical neutrino backgrounds to dark matter. Prompted by the latter, we estimated the projected sensitivities to general Lorentz invariant $X = \{S, P, V, A, T\}$ interactions through CE ν NS- and E ν ES-induced signals. With respect to light vector mediators, our study also considered the case of well-known U_{B-L} and $U_{L_\mu-L_\tau}$ anomaly-free models. To maximise the reliability of event rate simulations, important corrections from detector-specific quantities were taken into account such as the quenching factor and atomic binding effects for the case of CE ν NS and E ν ES, respectively. Our statistical analysis was performed under the assumption of a conservative scenario, including a flat background normalisation of the order of 10% with respect to the neutrino-induced signal and a 10% statistical uncertainty. We furthermore considered a minimal exposure of 1 ton \cdot yr which is readily achievable by the current and future xenon detector technologies. Our present results imply that future CE ν NS or E ν ES measurements at a direct detection dark matter experiment will not only become sensitive to neutrinos coming (mainly) from the sun, but will also offer competitive constraints to existing ones from dedicated CE ν NS and E ν ES experiments. We have furthermore illustrated that the expected sensitivities will cover a large part of the parameter space, previously unexplored from collider probes and beam dump experiments, improving upon the existing bounds by about one order of magnitude.

ACKNOWLEDGMENTS

The authors are indebted to D. Aristizabal-Sierra for carefully reading the manuscript and for insightful comments. The authors also acknowledge P. Martínez-Miravé for useful correspondence. The research of DKP is co-financed by Greece and the European Union (European Social Fund- ESF) through the Operational Programme “Human Resources Development, Education and Lifelong Learning” in the context of the project “Reinforcement of Postdoctoral Researchers - 2nd Cycle” (MIS-5033021), implemented by the State Scholarships Foundation (IKY). The work of RS is supported by the SERB, Government of India grant SRG/2020/002303.

-
- [1] P. Langacker, “The Physics of Heavy Z' Gauge Bosons,” *Rev.Mod.Phys.* **81** (2009) 1199–1228, [arXiv:0801.1345 \[hep-ph\]](#).

- [2] M. Dittmar, A.-S. Nicollerat, and A. Djouadi, “Z-prime studies at the LHC: An Update,” *Phys.Lett.B* **583** (2004) 111–120, [arXiv:hep-ph/0307020](#) [hep-ph].
- [3] **Muon g-2** Collaboration, B. Abi *et al.*, “Measurement of the Positive Muon Anomalous Magnetic Moment to 0.46 ppm,” *Phys. Rev. Lett.* **126** no. 14, (2021) 141801, [arXiv:2104.03281](#) [hep-ex].
- [4] T. Aoyama *et al.*, “The anomalous magnetic moment of the muon in the Standard Model,” *Phys.Rept.* **887** (2020) 1–166, [arXiv:2006.04822](#) [hep-ph].
- [5] P. Agrawal *et al.*, “Feebly-interacting particles: FIPs 2020 workshop report,” *Eur. Phys. J. C* **81** no. 11, (2021) 1015, [arXiv:2102.12143](#) [hep-ph].
- [6] M. Fabbrihesi, E. Gabrielli, and G. Lanfranchi, “The Dark Photon,” [arXiv:2005.01515](#) [hep-ph].
- [7] C. Boehm, D. G. Cerdeno, M. Fairbairn, P. A. Machado, and A. C. Vincent, “Light new physics in XENON1T,” *Phys.Rev.* **D102** (2020) 115013, [arXiv:2006.11250](#) [hep-ph].
- [8] D. Aristizabal Sierra, V. De Romeri, L. J. Flores, and D. K. Papoulias, “Light vector mediators facing XENON1T data,” *Phys. Lett. B* **809** (2020) 135681, [arXiv:2006.12457](#) [hep-ph].
- [9] A. N. Khan, “Can Nonstandard Neutrino Interactions explain the XENON1T spectral excess?,” *Phys. Lett. B* **809** (2020) 135782, [arXiv:2006.12887](#) [hep-ph].
- [10] R. D. Peccei and H. R. Quinn, “CP Conservation in the Presence of Instantons,” *Phys. Rev. Lett.* **38** (1977) 1440–1443.
- [11] S. Weinberg, “A New Light Boson?,” *Phys. Rev. Lett.* **40** (1978) 223–226.
- [12] F. Wilczek, “Problem of Strong P and T Invariance in the Presence of Instantons,” *Phys. Rev. Lett.* **40** (1978) 279–282.
- [13] J. Schechter and J. W. F. Valle, “Neutrino Decay and Spontaneous Violation of Lepton Number,” *Phys. Rev. D* **25** (1982) 774.
- [14] C. Bonilla, S. Centelles-Chuliá, R. Cepedello, E. Peinado, and R. Srivastava, “Dark matter stability and Dirac neutrinos using only Standard Model symmetries,” *Phys. Rev. D* **101** no. 3, (2020) 033011, [arXiv:1812.01599](#) [hep-ph].
- [15] D. G. Cerdeño, M. Fairbairn, T. Jubb, P. A. N. Machado, A. C. Vincent, and C. Boehm, “Physics from solar neutrinos in dark matter direct detection experiments,” *JHEP* **05** (2016) 118, [arXiv:1604.01025](#) [hep-ph]. [Erratum: JHEP 09, 048 (2016)].
- [16] E. Bertuzzo, F. F. Deppisch, S. Kulkarni, Y. F. Perez Gonzalez, and R. Zukanovich Funchal, “Dark Matter and Exotic Neutrino Interactions in Direct Detection Searches,” *JHEP* **1704** (2017) 073, [arXiv:1701.07443](#) [hep-ph].

- [17] **COHERENT** Collaboration, D. Akimov *et al.*, “Observation of Coherent Elastic Neutrino-Nucleus Scattering,” *Science* **357** no. 6356, (2017) 1123–1126, [arXiv:1708.01294 \[nucl-ex\]](#).
- [18] **COHERENT** Collaboration, D. Akimov *et al.*, “First Measurement of Coherent Elastic Neutrino-Nucleus Scattering on Argon,” *Phys. Rev. Lett.* **126** no. 1, (2021) 012002, [arXiv:2003.10630 \[nucl-ex\]](#).
- [19] D. Akimov *et al.*, “Measurement of the Coherent Elastic Neutrino-Nucleus Scattering Cross Section on CsI by COHERENT,” [arXiv:2110.07730 \[hep-ex\]](#).
- [20] J. B. Dent, B. Dutta, S. Liao, J. L. Newstead, L. E. Strigari, and J. W. Walker, “Probing light mediators at ultralow threshold energies with coherent elastic neutrino-nucleus scattering,” *Phys.Rev.* **D96** (2017) 095007, [arXiv:1612.06350 \[hep-ph\]](#).
- [21] J. Liao and D. Marfatia, “COHERENT constraints on nonstandard neutrino interactions,” *Phys.Lett.* **B775** (2017) 54–57, [arXiv:1708.04255 \[hep-ph\]](#).
- [22] Y. Farzan, M. Lindner, W. Rodejohann, and X.-J. Xu, “Probing neutrino coupling to a light scalar with coherent neutrino scattering,” *JHEP* **1805** (2018) 066, [arXiv:1802.05171 \[hep-ph\]](#).
- [23] D. K. Papoulias, “COHERENT constraints after the COHERENT-2020 quenching factor measurement,” *Phys.Rev.* **D102** (2020) 113004, [arXiv:1907.11644 \[hep-ph\]](#).
- [24] B. Dutta, S. Liao, S. Sinha, and L. E. Strigari, “Searching for Beyond the Standard Model Physics with COHERENT Energy and Timing Data,” *Phys.Rev.Lett.* **123** (2019) 061801, [arXiv:1903.10666 \[hep-ph\]](#).
- [25] D. Aristizabal Sierra, B. Dutta, S. Liao, and L. E. Strigari, “Coherent elastic neutrino-nucleus scattering in multi-ton scale dark matter experiments: Classification of vector and scalar interactions new physics signals,” *JHEP* **1912** (2019) 124, [arXiv:1910.12437 \[hep-ph\]](#).
- [26] O. Miranda, D. Papoulias, G. Sanchez Garcia, O. Sanders, M. Tórtola, and J. Valle, “Implications of the first detection of coherent elastic neutrino-nucleus scattering (CEvNS) with Liquid Argon,” *JHEP* **2005** (2020) 130, [arXiv:2003.12050 \[hep-ph\]](#).
- [27] M. Cadeddu, N. Cargioli, F. Dordei, C. Giunti, Y. F. Li, E. Picciau, and Y. Y. Zhang, “Constraints on light vector mediators through coherent elastic neutrino nucleus scattering data from COHERENT,” *JHEP* **01** (2021) 116, [arXiv:2008.05022 \[hep-ph\]](#).
- [28] **CONNIE** Collaboration, A. Aguilar-Arevalo *et al.*, “Search for light mediators in the low-energy data of the CONNIE reactor neutrino experiment,” *JHEP* **04** (2020) 054, [arXiv:1910.04951 \[hep-ex\]](#).

- [29] **CONUS** Collaboration, H. Bonet *et al.*, “Novel constraints on neutrino physics beyond the standard model from the CONUS experiment,” [arXiv:2110.02174 \[hep-ph\]](#).
- [30] D. W. P. d. Amaral, D. G. Cerdeno, P. Foldenauer, and E. Reid, “Solar neutrino probes of the muon anomalous magnetic moment in the gauged $U(1)_{L_\mu-L_\tau}$,” *JHEP* **12** (2020) 155, [arXiv:2006.11225 \[hep-ph\]](#).
- [31] D. Amaral, D. Cerdeno, A. Cheek, and P. Foldenauer, “Confirming $U(1)_{L_\mu-L_\tau}$ as a solution for $(g-2)_\mu$ with neutrinos,” *Eur.Phys.J.C* **81** (2021) 861, [arXiv:2104.03297 \[hep-ph\]](#).
- [32] D. G. Cerdeño, M. Cernero, M. Á. Pérez-García, and E. Reid, “Medium effects in supernovae constraints on light mediators,” *Phys.Rev.D* **104** (2021) 063013, [arXiv:2106.11660 \[hep-ph\]](#).
- [33] D. Aristizabal Sierra, V. De Romeri, L. Flores, and D. Papoulias, “Impact of COHERENT measurements, cross section uncertainties and new interactions on the neutrino floor,” [arXiv:2109.03247 \[hep-ph\]](#).
- [34] D. Aristizabal Sierra, V. De Romeri, and N. Rojas, “COHERENT analysis of neutrino generalized interactions,” *Phys.Rev.* **D98** (2018) 075018, [arXiv:1806.07424 \[hep-ph\]](#).
- [35] A. N. Khan, W. Rodejohann, and X.-J. Xu, “Borexino and general neutrino interactions,” *Phys.Rev.D* **101** (2020) 055047, [arXiv:1906.12102 \[hep-ph\]](#).
- [36] F. Escrivuela, L. Flores, O. Miranda, and J. Rendón, “Global constraints on neutral-current generalized neutrino interactions,” *JHEP* **07** (2021) 061, [arXiv:2105.06484 \[hep-ph\]](#).
- [37] W. Rodejohann, X.-J. Xu, and C. E. Yaguna, “Distinguishing between Dirac and Majorana neutrinos in the presence of general interactions,” *JHEP* **05** (2017) 024, [arXiv:1702.05721 \[hep-ph\]](#).
- [38] J. Barranco, A. Bolanos, E. Garces, O. Miranda, and T. Rashba, “Tensorial NSI and Unparticle physics in neutrino scattering,” *Int.J.Mod.Phys.A* **27** (2012) 1250147, [arXiv:1108.1220 \[hep-ph\]](#).
- [39] D. Papoulias and T. Kosmas, “Neutrino transition magnetic moments within the non-standard neutrino–nucleus interactions,” *Phys.Lett.* **B747** (2015) 454–459, [arXiv:1506.05406 \[hep-ph\]](#).
- [40] D. K. Papoulias and T. S. Kosmas, “COHERENT constraints to conventional and exotic neutrino physics,” *Phys. Rev. D* **97** no. 3, (2018) 033003, [arXiv:1711.09773 \[hep-ph\]](#).
- [41] **XENON** Collaboration, E. Aprile *et al.*, “Search for Coherent Elastic Scattering of Solar ^8B Neutrinos in the XENON1T Dark Matter Experiment,” *Phys. Rev. Lett.* **126** (2021) 091301, [arXiv:2012.02846 \[hep-ex\]](#).
- [42] **XENON** Collaboration, E. Aprile *et al.*, “Projected WIMP sensitivity of the XENONnT dark matter experiment,” *JCAP* **11** (2020) 031, [arXiv:2007.08796 \[physics.ins-det\]](#).

- [43] J. Barranco, O. Miranda, and T. Rashba, “Probing new physics with coherent neutrino scattering off nuclei,” *JHEP* **0512** (2005) 021.
- [44] O. Tomalak, P. Machado, V. Pandey, and R. Plestid, “Flavor-dependent radiative corrections in coherent elastic neutrino-nucleus scattering,” *JHEP* **02** (2021) 097, [arXiv:2011.05960 \[hep-ph\]](#).
- [45] D. Aristizabal Sierra, R. Branada, O. G. Miranda, and G. Sanchez Garcia, “Sensitivity of direct detection experiments to neutrino magnetic dipole moments,” *JHEP* **12** (2020) 178, [arXiv:2008.05080 \[hep-ph\]](#).
- [46] D. K. Papoulias, R. Sahu, T. S. Kosmas, V. K. B. Kota, and B. Nayak, “Novel neutrino-floor and dark matter searches with deformed shell model calculations,” *Adv. High Energy Phys.* **2018** (2018) 6031362, [arXiv:1804.11319 \[hep-ph\]](#).
- [47] D. K. Papoulias and T. S. Kosmas, “Standard and Nonstandard Neutrino-Nucleus Reactions Cross Sections and Event Rates to Neutrino Detection Experiments,” *Adv. High Energy Phys.* **2015** (2015) 763648, [arXiv:1502.02928 \[nucl-th\]](#).
- [48] R. H. Helm, “Inelastic and Elastic Scattering of 187-Mev Electrons from Selected Even-Even Nuclei,” *Phys.Rev.* **104** (1956) 1466–1475.
- [49] M. Lindner, W. Rodejohann, and X.-J. Xu, “Coherent Neutrino-Nucleus Scattering and new Neutrino Interactions,” *JHEP* **1703** (2017) 097, [arXiv:1612.04150 \[hep-ph\]](#).
- [50] K. R. Dienes, J. Kumar, B. Thomas, and D. Yaylali, “Overcoming Velocity Suppression in Dark-Matter Direct-Detection Experiments,” *Phys.Rev.D* **90** (2014) 015012, [arXiv:1312.7772 \[hep-ph\]](#).
- [51] M. Cirelli, E. Del Nobile, and P. Panci, “Tools for model-independent bounds in direct dark matter searches,” *JCAP* **10** (2013) 019, [arXiv:1307.5955 \[hep-ph\]](#).
- [52] M. Fauzi, *talk at BSM-2021*, 2021.
<https://indico.cern.ch/event/959266/contributions/4237944/>.
- [53] D. Aristizabal Sierra, J. Liao, and D. Marfatia, “Impact of form factor uncertainties on interpretations of coherent elastic neutrino-nucleus scattering data,” *JHEP* **06** (2019) 141, [arXiv:1902.07398 \[hep-ph\]](#).
- [54] Y. Ema, F. Sala, and R. Sato, “Neutrino experiments probe hadrophilic light dark matter,” *SciPost Phys.* **10** (2021) 72. <https://scipost.org/10.21468/SciPostPhys.10.3.072>.
- [55] J. Ellis, K. A. Olive, and C. Savage, “Hadronic uncertainties in the elastic scattering of supersymmetric dark matter,” *Phys. Rev. D* **77** (Mar, 2008) 065026.
<https://link.aps.org/doi/10.1103/PhysRevD.77.065026>.
- [56] M. Hoferichter, J. Menéndez, and A. Schwenk, “Coherent elastic neutrino-nucleus scattering: EFT analysis and nuclear responses,” *Phys. Rev. D* **102** no. 7, (2020) 074018,

- [arXiv:2007.08529 \[hep-ph\]](#).
- [57] H.-Y. Cheng, “Low-energy Interactions of Scalar and Pseudoscalar Higgs Bosons With Baryons,” *Phys.Lett.B* **219** (1989) 347–353.
 - [58] H.-Y. Cheng and C.-W. Chiang, “Revisiting Scalar and Pseudoscalar Couplings with Nucleons,” *JHEP* **07** (2012) 009, [arXiv:1202.1292 \[hep-ph\]](#).
 - [59] L. Flores, N. Nath, and E. Peinado, “Non-standard neutrino interactions in $U(1)'$ model after COHERENT data,” *JHEP* **2006** (2020) 045, [arXiv:2002.12342 \[hep-ph\]](#).
 - [60] W. Altmannshofer, S. Gori, J. Martín-Albo, A. Sousa, and M. Wallbank, “Neutrino Tridents at DUNE,” *Phys.Rev.D* **100** (2019) 115029, [arXiv:1902.06765 \[hep-ph\]](#).
 - [61] L. M. de la Vega, L. Flores, N. Nath, and E. Peinado, “Complementarity between dark matter direct searches and $CE\nu NS$ experiments in $U(1)'$ models,” *JHEP* **09** (2021) 146, [arXiv:2107.04037 \[hep-ph\]](#).
 - [62] C. Giunti and C. W. Kim, *Fundamentals of Neutrino Physics and Astrophysics*. 2007.
 - [63] B. Kayser, E. Fischbach, S. P. Rosen, and H. Spivack, “Charged and Neutral Current Interference in $\nu_e e$ Scattering,” *Phys.Rev.D* **20** (1979) 87.
 - [64] M. Lindner, F. S. Queiroz, W. Rodejohann, and X.-J. Xu, “Neutrino-electron scattering: general constraints on Z' and dark photon models,” *JHEP* **1805** (2018) 098, [arXiv:1803.00060 \[hep-ph\]](#).
 - [65] P. Ballett *et al.*, “ Z' s in neutrino scattering at DUNE,” *Phys.Rev.D* **100** (2019) 055012, [arXiv:1902.08579 \[hep-ph\]](#).
 - [66] J. M. Link and X.-J. Xu, “Searching for BSM neutrino interactions in dark matter detectors,” *JHEP* **08** (2019) 004, [arXiv:1903.09891 \[hep-ph\]](#).
 - [67] W. Haxton, R. Hamish Robertson, and A. M. Serenelli, “Solar Neutrinos: Status and Prospects,” *Ann.Rev.Astron.Astrophys.* **51** (2013) 21–61, [arXiv:1208.5723 \[astro-ph.SR\]](#).
 - [68] G. Battistoni, A. Ferrari, T. Montaruli, and P. Sala, “The atmospheric neutrino flux below 100-MeV: The FLUKA results,” *Astropart.Phys.* **23** (2005) 526–534.
 - [69] J. F. Beacom, “The Diffuse Supernova Neutrino Background,” *Ann.Rev.Nucl.Part.Sci.* **60** (2010) 439–462, [arXiv:1004.3311 \[astro-ph.HE\]](#).
 - [70] J. Monroe and P. Fisher, “Neutrino Backgrounds to Dark Matter Searches,” *Phys. Rev. D* **76** (2007) 033007, [arXiv:0706.3019 \[astro-ph\]](#).
 - [71] G. B. Gelmini, V. Takhistov, and S. J. Witte, “Geoneutrinos in Large Direct Detection Experiments,” *Phys.Rev.D* **99** (2019) 093009, [arXiv:1812.05550 \[hep-ph\]](#).
 - [72] T. Kosmas, V. Kota, D. Papoulias, and R. Sahu, “Coherent elastic neutrino-nucleus scattering ($CE\nu NS$) event rates for Ge, Zn and Si detector materials,” [arXiv:2111.08488 \[nucl-th\]](#).

- [73] D. Baxter *et al.*, “Recommended conventions for reporting results from direct dark matter searches,” *Eur.Phys.J.C* **81** (2021) 907, [arXiv:2105.00599 \[hep-ex\]](#).
- [74] J. Lewin and P. Smith, “Review of mathematics, numerical factors, and corrections for dark matter experiments based on elastic nuclear recoil,” *Astropart.Phys.* **6** (1996) 87–112.
- [75] J. Lindhard, M. Scharff, and H. Schiott, “Range concepts and heavy ion searches,” *Mat. Fys. Medd . Dan. Vid. Selsk.* **33** (1963) .
- [76] B. Scholz, A. Chavarria, J. Collar, P. Privitera, and A. Robinson, “Measurement of the low-energy quenching factor in germanium using an $^{88}\text{Y}/\text{Be}$ photoneutron source,” *Phys.Rev.D* **94** (2016) 122003, [arXiv:1608.03588 \[physics.ins-det\]](#).
- [77] Y. Sarkis, A. Aguilar-Arevalo, and J. C. D’Olivo, “Study of the ionization efficiency for nuclear recoils in pure crystals,” *Phys.Rev.D* **101** (2020) 102001, [arXiv:2001.06503 \[hep-ph\]](#).
- [78] D. Aristizabal Sierra, N. Rojas, and M. Tytgat, “Neutrino non-standard interactions and dark matter searches with multi-ton scale detectors,” *JHEP* **1803** (2018) 197, [arXiv:1712.09667 \[hep-ph\]](#).
- [79] F. Escrivuela, O. Miranda, M. Tortola, and J. Valle, “Constraining nonstandard neutrino-quark interactions with solar, reactor and accelerator data,” *Phys.Rev.D* **80** (2009) 105009, [arXiv:0907.2630 \[hep-ph\]](#).
- [80] P. de Salas *et al.*, “2020 global reassessment of the neutrino oscillation picture,” *JHEP* **02** (2021) 071, [arXiv:2006.11237 \[hep-ph\]](#).
- [81] J.-W. Chen, H.-C. Chi, C. P. Liu, and C.-P. Wu, “Low-energy electronic recoil in xenon detectors by solar neutrinos,” *Phys. Lett. B* **774** (2017) 656–661, [arXiv:1610.04177 \[hep-ex\]](#).
- [82] R. Sahu, D. Papoulias, V. Kota, and T. Kosmas, “Elastic and inelastic scattering of neutrinos and weakly interacting massive particles on nuclei,” *Phys.Rev.* **C102** (2020) 035501, [arXiv:2004.04055 \[nucl-th\]](#).
- [83] **XENON** Collaboration, E. Aprile *et al.*, “Excess electronic recoil events in XENON1T,” *Phys. Rev. D* **102** no. 7, (2020) 072004, [arXiv:2006.09721 \[hep-ex\]](#).
- [84] A. Friedland, C. Lunardini, and M. Maltoni, “Atmospheric neutrinos as probes of neutrino-matter interactions,” *Phys.Rev.* **D70** (2004) 111301.
- [85] **ATLAS** Collaboration, M. Aaboud *et al.*, “Search for high-mass new phenomena in the dilepton final state using proton-proton collisions at $\sqrt{s} = 13$ TeV with the ATLAS detector,” *Phys.Lett.* **B761** (2016) 372–392, [arXiv:1607.03669 \[hep-ex\]](#).
- [86] R. Harnik, J. Kopp, and P. A. Machado, “Exploring ν Signals in Dark Matter Detectors,” *JCAP* **1207** (2012) 026, [arXiv:1202.6073 \[hep-ph\]](#).

- [87] P. Ilten, Y. Soreq, M. Williams, and W. Xue, “Serendipity in dark photon searches,” *JHEP* **06** (2018) 004, [arXiv:1801.04847 \[hep-ph\]](#).
- [88] **BaBar** Collaboration, J. Lees *et al.*, “Search for a Dark Photon in e^+e^- Collisions at BaBar,” *Phys.Rev.Lett.* **113** (2014) 201801, [arXiv:1406.2980 \[hep-ex\]](#).
- [89] **BaBar** Collaboration, J. Lees *et al.*, “Search for Invisible Decays of a Dark Photon Produced in e^+e^- Collisions at BaBar,” *Phys.Rev.Lett.* **119** (2017) 131804, [arXiv:1702.03327 \[hep-ex\]](#).
- [90] **LHCb** Collaboration, R. Aaij *et al.*, “Search for Dark Photons Produced in 13 TeV pp Collisions,” *Phys.Rev.Lett.* **120** (2018) 061801, [arXiv:1710.02867 \[hep-ex\]](#).